Parametric analysis on drilling of aluminium alloy hybrid composites reinforced with SIC/WC

Engineering Research Express

CrossMark

OPEN ACCESS

RECEIVED
22 March 2022

REVISED
27 April 2022

ACCEPTED FOR PUBLICATION
16 May 2022

PUBLISHED
1 June 2022

PAPER

Parametric analysis on drilling of aluminium alloy hybrid composites reinforced with SIC/WC

S Senthil Babu[1], C Dhanasekaran[1], G Anbuchezhiyan[2] and Kumaran Palani[3]

[1] Department of Mechanical Engineering, Vels Institute of Science, Technology and Advanced Studies, Chennai-600117, Kancheepuram, Tamil Nadu, India

[2] Department of Mechanical Engineering, Saveetha School of Engineering, Saveetha Institute of Medical and Technical Sciences, Chennai-602105, Tamil Nadu, India

[3] Department of Mechanical Engineering, College of Engineering, Wolaita Sodo University, Wolaita Sodo, P.O. Box: 138, Ethiopia

E-mail: pkumaran2003@gmail.com and rssenthilbabu@gmail.com

Keywords: hybrid composites, stir casting, drilling, desirability analysis, ANN, regression modeling

Abstract

Aluminium alloy (Al7075) based hybrid metal matrix composites reinforced with Silicon carbide (SiC) and Tungsten carbide (WC), at 5 wt% each are considered for this investigation, which are developed by stir casting methodology. Material characteristic analysis both at micro and macro (Tensile strength and micro hardness) level were performed. This investigation is further progressed with drilling of the composites using titanium aluminium nitride coated carbide drill (5mm diameter) for varied point angle, feed rate and drill speed. The responses such as thrust force, surface roughness and roundness error were investigated by adopting Response Surface Methodology (RSM). Multiple linear regression (MLR) is developed along with Artificial Neural Networks (ANN) model for predicting the outputs. Scanning Electron Microscope (SEM) image reveals the uniform distribution of ceramic particles in matrix which ascertains enhanced mechanical properties. The parameters such as feed rate and point angle are found to have significant influence during drilling process. The roundness error is found higher with higher point angle which is due to the wider cutting edges in the drill bit. For unconstrained multi-objective optimization, the optimal condition obtained are 128°-point angle, 0.05 mm rev^{-1} feed rate and 1000 rpm drill speed. For constrained optimization (roundness error $\leqslant$0.05 mm), optimal conditions are 118° point angle, 0.05 mm rev^{-1} feed rate and 1000 rpm drill speed.

Abbreviations

SiC	Silicon carbide
WC	Tungsten carbide
TiAlN	Titanium aluminium nitride
RSM	Response Surface Methodology
ANN	Artificial Neural Networks
SEM	Scanning Electron Microscope
HAMMC	Hybrid aluminium metal matrix composites
ANOVA	Analysis of Variance
MLR	Multiple linear regression
MSE	Mean squared error

1. Introduction

For usage in marine and automotive sectors lightweight materials are needed, which is fabricated by the addition of ceramic particulates with suitable parent alloy material. With hard ceramic particles embedded in the matrix, machining becomes more tedious due to involvement of higher cutting forces and tool wear. Hence, machining of composite materials is very much in demand for high end engineering applications [1]. Hybrid intermixtures form a group of materials that have been attracted by number of researchers because of their improved properties when compared with monolithic materials. Attempts have been made to fabricate mechanical components using these composite materials; however, some measure of finishing should be done to complete the assembly process [2]. The metal removal mechanism in oblique machining like drilling, the variation in cutting forces and their influence on the damages caused in the cutting tool and work piece is most significant [3]. The drilling forces and damages caused can be minimized through proper selection of tool geometries and machining parameters [4]. In any case, for assembly and joining, drilling becomes a predominant machining process under demand. Because of the reinforcements, machining of hybrid composites became a challenging task in the production industries as various factors affect the quality of drilled characteristics [5]. Material removal rate, cutting forces, circularity and roundness error and surface roughness have been observed in drilling hybrid aluminium alloy metal matrix composite (HAMMC), that are affected by various parameters like drill point angle, speed and tool material [6].

The cryogenic machining nano-SiC reinforced aluminium composite using dry machining and minimum quantity lubrication (MQL) using carbide drills of different point angles based on Box-Behnken design (BBD) design of RSM and Teaching-Learning based optimization (TLBO) and found that, cushioning effect and improved lubrication from cryogenic machining improves machining performance [7]. Also, nano filled improves the drilling condition through higher ball-bearing effect. The investigation machining behavior of Al7075 + SiC composite using high-speed steel (HSS) drill bit and HSS drill coated with titanium nitride (TiN) drills and found that, rate of feed and spindle speed influences roughness of hole surface, which elevates with higher rate of feed and lowers at higher drill speeds [8]. The drill damage on roundness error during drilling glass fiber reinforced polypropylene (GFR/PP) using solid carbide spur and brad drills by adopting BBD design of RSM and found that, roundness error elevates with higher diameter of drill and feed rate. The developed empirical models with 95% confidence interval could effectively predict the roundness error [9].

The cutting forces during dry drilling of aluminium composites using neural network with feed forward back propagation algorithm and found that absolute error is 2.03% and 3.46% among predicted and experimental torque and thrust force [10]. The drilling experiments and measured circularity, roughness and cylindricity of holes on silicon nitride composites by altering feed and speed. They also analyzed the results with ANN model and found it a reliable method for prediction [11]. The investigation on the effect of drilling factors on cutting forces for hybrid composites with multiple regression and ANN for prediction, found that ANN showed better prediction than MRA [12]. Babu *et al* The impact of drilling variables on roughness of drilled holes and compared with the predicted values by Fuzzy Logic and concluded that the results were close to each other [13]. The drilled hybrid composites with carbide drill coated with TiAlN and concluded that the drill material is most significant than speed and feed, and also suggested that the TiAlN coated drill showed the best performance among the various drill tool materials [14]. The hybrid metal matrix composites with particulate boron carbide reinforcement possess a good combination of good elastic property, specific strength, high thermal stability and excellent wear resistance. The machining studies on HAMMC fabricated through powder metallurgy technique by adopting Taguchi's technique and optimized the inputs using grey relational analysis a non-dominated sorting genetic algorithm [15].

From the survey, it is identified that, limited investigations were done on machining of hybrid aluminium metal matrix composites (HAMMC) reinforced with primary (SiC) and secondary (WC) ceramic particulates due to the difficulties in wettability and economic constraints. Hence, performing drilling studies on the fabricated HAMMC using coated (TiAlN) carbide drill with three different point angle, feed rate and drilling speeds is considered novel in this investigation. Experimentations are planned and analyzed using response surface methodology technique (RSM).Both unconstrained and constrained optimization is done. Prediction of output responses is done using empirical models developed from MLR and from ANN model and subsequently the outcomes are compared.

2. Fabrication and experimental methods

A stir casting process can be used to fabricate aluminum matrix composites and hybrid aluminum matrix composites since it is an economical process that is ideal for mass production [16]. As the aluminum melt reacts with the atmosphere and moisture, aluminum oxide forms a protective layer over the melting surface that

Table 1. Drilling factors and their values.

Drilling parameter	Level 1	Level 2	Level 3
Point angle (°)	108	118	128
Feed rate (mm rev^{-1})	0.05	0.1	0.15
Drill speed (rpm)	1000	2000	3000

shields the melt from further atmospheric reactions and hence it prevents causing serious damage from atmosphere [17]. By considering this in the present study Fabrication of composites is done by stir-casting technique, which is a liquid state technique for preparing the composites in an economical manner in which the reinforced materials are blended together with the liquid aluminium (Al7075) matrix by stirring it mechanically [18]. Small pieces of Al7075 bar is placed and melted in a crucible made of graphite. The reinforcement materials are preheated separately and blended with molten slurry consistently utilizing a ceramic stirrer attached to electric motor running at 300rpm for a period of 10 min followed by which the molten slurry is then transferred to the mould cavity for solidification at room temperature. The ceramic strengthening particulates of SiC and WC are added to the melt through the external sprue in amounts of 5wt% each. To get a homogeneous distribution of reinforcement in the matrix materials, the stirring speed and stirring time was kept at 500 rpm and 15 min, respectively [19]. When the ceramic particulates were added to the molten alloy, unwetted particles caused the particles to float on the surface, even after the reinforcing particles were mixed mechanically. The particles tended to return to the surface when stirring ceased, and most of the particles were still stuck together. In casting, a minimum amount of porosity is present. By increasing the particle percentage in the matrix, more porosity was formed as a result of SiO_2 layer cladding the ceramic particles, which put out moisture when particles were introduced [20]. Upon pouring the molten slurry into the die cavity, the molten slurry was allowed to cool at room temperature.

2.1. Taguchi's design of experiments

Taguchi's technique for parametric design is adopted for enhancing the system robustness, thereby assisting in decisions during process and product designs [21]. For process variable optimization, this procedure can be adopted due to its simplicity and adaptability [22]. This procedure delivers the required information from least experimental trials with various levels of input conditions [23]. With three factors varied at three levels, considering the interaction effects among them, Taguchi's methodology is chosen, consecutively a L27 orthogonal array (OA) is selected. It is apprehended that OA based design characterizes the least likely section of all probable combinations [24]. The minimal experimental trial that provide satisfactory outcomes are the two prime aspects that OAs are chosen for investigational designs. The validation of results arises from carrying out experiments with real conditions and by performing confirmation tests with optimal condition [25]. The drilling parameters as shown in table 1 are analyzed for improving the performance by identifying an optimal drilling condition.

2.2. Response surface methodology

Response Surface Methodology (RSM) associates the procedures of statistical tools and optimization through appropriate model [26] RSM is usually projected for identifying the ideal condition after initial screening where the responses are related only towards the significant input parameters. The results obtained are applied suitably for performing experimental investigation by adopting RSM through the inclusion of replications of data points, with the development of a suitable empirical model [27]. For m input factors x1, x2… xm, the effective association between the output response and m input conditions be represented as:

$$\eta = f(x_1, x_2, \ldots\ldots x_m) \tag{1}$$

3. Results and discussion

SEM images reveals the homogenous distribution of strengthening particulates in the base materials, without indication of residual pore. Due to higher temperature characteristics the strengthening particles cannot be solidified in the matrix alloy and hence appears as globular particles in parent material [28]. The matrix shows the large grains with some Mg_2Si precipitation and little amount of un-dissolved Al_6 (Fe, Mn) in solid solution of aluminium.

From XRD analysis it is clearly inferred that the base material aluminium alloy occupies a peak factor and followed by the strengthening particulates. The peak factors of synthesized composites that are obtained from

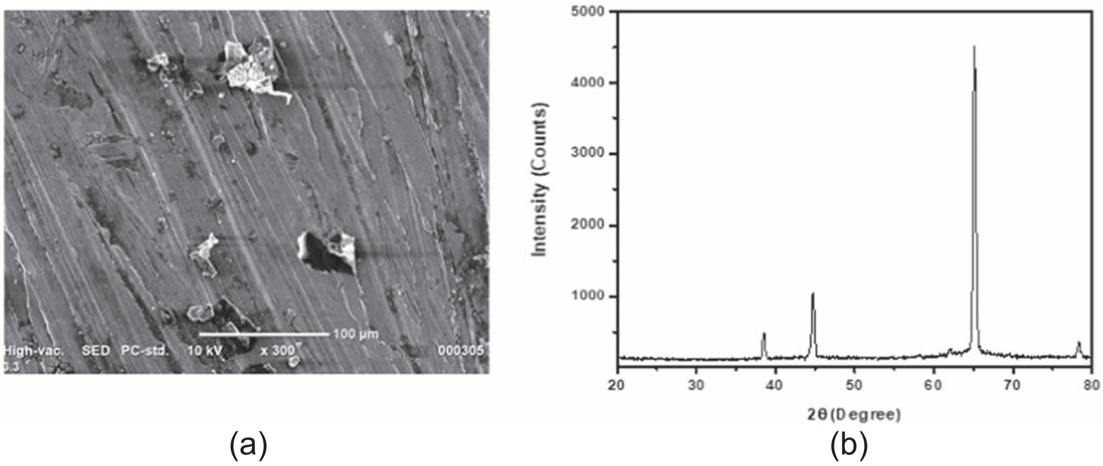

Figure 1. SEM and XRD of HAMMC.

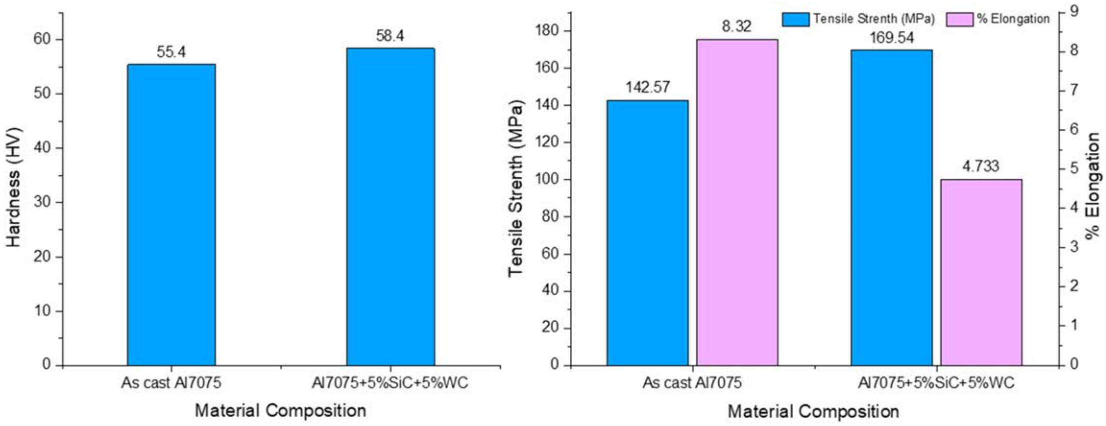

Figure 2. Tensile and micro-hardness of cast composite.

the XRD are Al (33.2°, 36.3°, 38.2°, 48.5°), SiC (34.2°, 58.6°, 64.2°) and WC (28.6°, 38.6°, 46.8°, 68.2°) at 2θ respectively as shown in figures 1(a)–(b).

The Tensile strength is determined for the as cast Al7075 and HAMMC as per ASTM-E8 standard and micro-hardness as per ASTM-E384 standard [29]. It is observed from the figure 2 that, with inclusio n of ceramic particles, improvement is found in micro-hardness and tensile strength [30]. With increase in tensile strength the % elongation tends to reduce due to lowering of ductility of the HAMMC, ceramic particles hindering the dislocation motion of cracks during the tensile test.

Using CNC based vertical machining centre, drilling experiments has been done. To record the thrust force, Kistler dynamometer has been used. Kosaka—Surf coder SE700 is used for measuring the drilled hole roughness value. Roundness error has been evaluated for all the holes using coordinate measuring machine [31]. The SEM Image of drilled composites samples is shown in figure 3.

As per L27 OA, machining tests are performed in HAMMC using traditional drilling process. Table 2 displays the outcomes of experimentation for all 27 tests with TiAlN coated carbide tool [32] of diameter 5 mm.

From investigational outcomes, thrust force are found to be higher for increasing point angle [33] Roughness in drilled hole is least for drill bit with point angle of 118° due to less removal of chip area, whereas roundness error tends to increase with increasing point angle. The significance of rate of feed on thrust force and roundness error was higher [34], roundness error and thrust force tends to increase with increasing rate of feed but surface roughness tends to reduce for 0.1 mm rev^{-1} and further rise to 0.15 mm rev^{-1}, surface roughness increases as more amount of material is removed. Drill speed influences thrust force [35] and roundness error [36]. With higher speeds, vibration takes places and hence increases the roundness error. With higher drilling speed, surface roughness tends to increase [37].

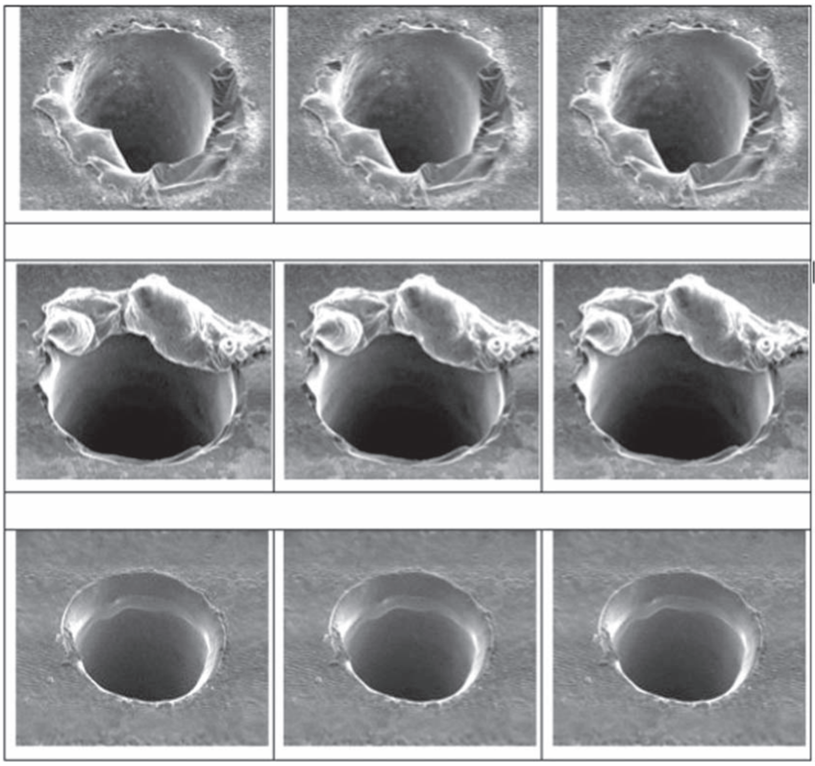

Figure 3. Drilled hole of Aluminium hybrid composites.

Table 2. Experimental outcomes.

Expt.No	Point angle °	Feed mm rev^{-1}	Speed rpm	Thrust Force (N)	Surface roughness (μm)	Roundness error (mm)
1	108	0.05	1000	43.027	10.352	0.0278
2	108	0.05	2000	97.839	10.986	0.0313
3	108	0.05	3000	161.588	9.658	0.04
4	108	0.1	1000	90.084	9.717	0.024
5	108	0.1	2000	169.093	10.51	0.0312
6	108	0.1	3000	257.041	9.341	0.0436
7	108	0.15	1000	123.843	10.37	0.0316
8	108	0.15	2000	227.050	11.322	0.0425
9	108	0.15	3000	339.196	10.312	0.0586
10	118	0.05	1000	110.091	6.996	0.0498
11	118	0.05	2000	154.252	7.818	0.0531
12	118	0.05	3000	207.350	6.678	0.0616
13	118	0.1	1000	134.375	6.193	0.0547
14	118	0.1	2000	202.734	7.174	0.0617
15	118	0.1	3000	280.030	6.193	0.0739
16	118	0.15	1000	145.361	6.678	0.071
17	118	0.15	2000	237.917	7.818	0.0817
18	118	0.15	3000	339.412	6.996	0.0976
19	128	0.05	1000	77.829	8.486	0.0152
20	128	0.05	2000	111.339	9.496	0.0183
21	128	0.05	3000	153.787	8.544	0.0266
22	128	0.1	1000	79.340	7.515	0.0288
23	128	0.1	2000	137.047	8.684	0.0356
24	128	0.1	3000	203.693	7.891	0.0476
25	128	0.15	1000	67.552	7.832	0.0538
26	128	0.15	2000	149.458	9.16	0.0643
27	128	0.15	3000	240.302	8.526	0.08

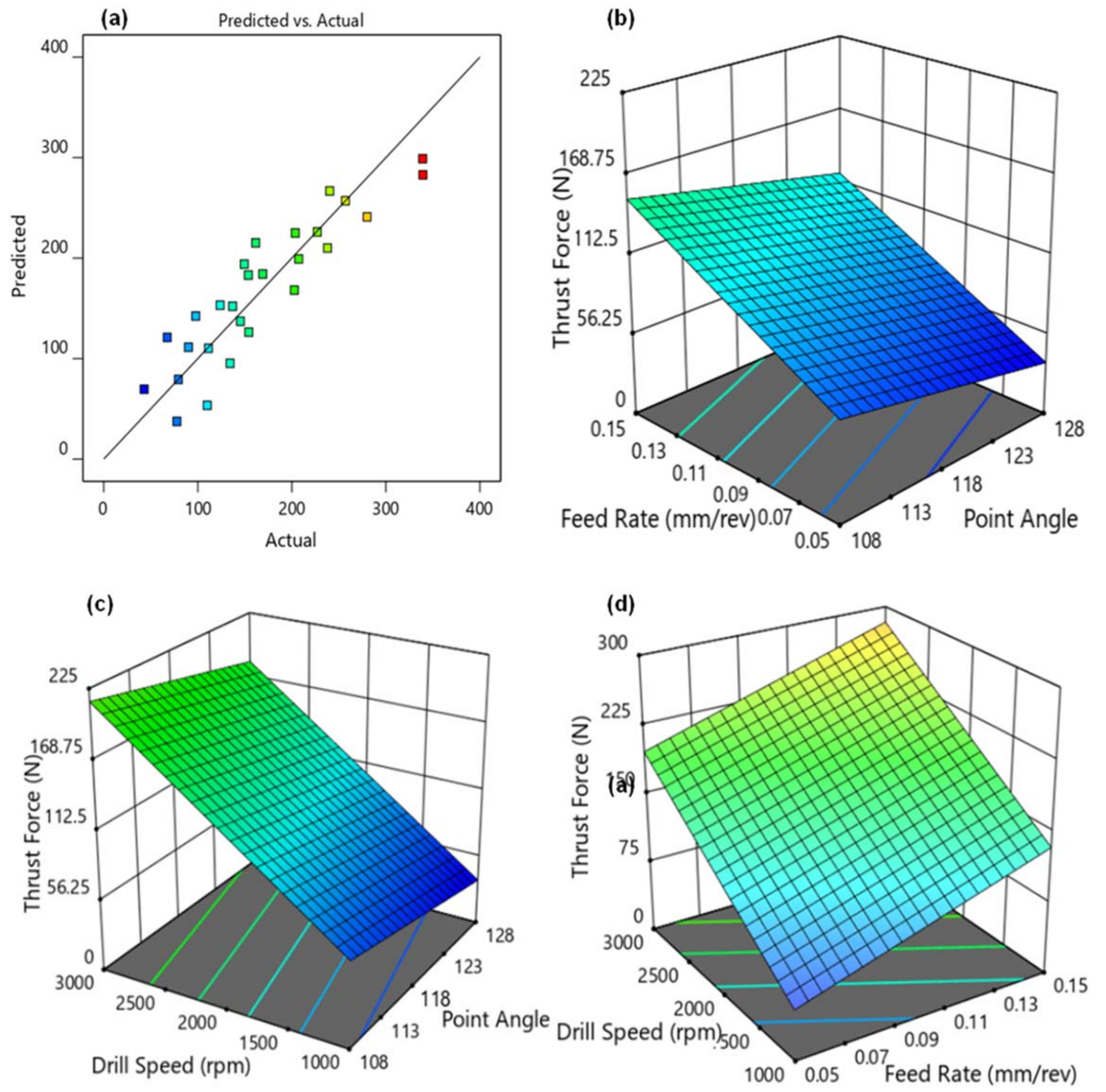

Figure 4. Diagnostic and model graphs for thrust force.

Table 3. ANOVA table for Thrust force.

Source	SS	DoF	MS	F-value	p-value	
Model	1.47E + 05	6	24462.33	33.48434	2.06E-09	significant
Point Angle	19419.81	2	9709.903	13.29103	0.000213	
Feed Rate	31764.83	2	15882.42	21.74005	9.64E-06	
Drill Speed	95589.33	2	47794.67	65.42193	1.68E-09	
Residual	14611.21	20	730.5603			
Cor Total	1.61E + 05	26				
Std. Dev.	27.02888		R^2	0.909464		
Mean	168.1715		Adjusted R^2	0.882303		
C.V.%	16.07221		Predicted R^2	0.834998		
			Adeq Precision	21.43566		

3.1. Analysis of thrust force

Thrust forces arising from drilling process due to friction contains significant information that are correlated to adequate generation of temperature towards improving quality of the product and lower wear of tools [38]. Thrust force acts along the spindle axis and in the direction of drill feed. Thrust force is greatly affected by the drilling tool lips and the major contributor to thrust force is the chisel edge [39].

Table 4. ANOVA table for surface roughness.

Source	SS	DoF	MS	F-value	p-value	
Model	58.49	6	9.75	182.87	< 0.0001	significant
Point Angle	50.23	2	25.11	471.12	< 0.0001	
Feed Rate	2.49	2	1.24	23.34	< 0.0001	
Drill Speed	5.77	2	2.89	54.16	< 0.0001	
Residual	1.07	20	0.0533			
Cor Total	59.56	26				
Std. Dev.	0.230888		R^2	0.982099		
Mean	8.564667		Adjusted R^2	0.976728		
C.V.%	2.695823		Predicted R^2	0.967375		
			Adeq Precision	42.19881		

Statistical tool, Analysis of Variance (ANOVA) is used to identify the significant influence of independent variables over the dependent variables by determining the variance among the selected input parametersm [40]. By adopting response surface design, the measured thrust force is analyzed and the ANOVA table obtained is presented in table 3, which shows that a significant linear model is developed with an R2 value of 90.94%. The contribution of drill speed is 59.37% towards the produced thrust force, followed by feed rate (19.73%) and point angle by 12.06% [41]. Probability values lower than 0.05 specify significant terms in model, here all the considered inputs are significant model terms. Adequate precision value determines adequate signal with lower noise levels. Generally, the desired signal-to-noise (S/N) ratio higher than 4 is required, here 21.436 shows a satisfactory signal.

A graph drawn between predicted and actual values of a response is actual versus predicted plot, which is used to distinguish data's that cannot be predicted well by the developed model. This scatter plot is the best method of visualizing the data, with most of the points closer to the diagonal line formed indicating the obtained responses are linear in nature. Model developed with higher R2 value provides all data points closer to the formed diagonal line.

Response surface plots are beneficial for creating necessary operating situations and responses. Surface plot usually exhibits a 3D view providing a distinctive nature of the output response. For first order empirical model is framed considering main effects only, the response surface fitted is a plane with straight contour lines. If interaction is considered in the fitted model, curved contour line is formed and the response surface will be non-linear [42].

In figure 4(a), the predicted versus actual graph, all the dispersed points are scattered on both sides of the 45° diagonal line and hence it can be stated that, a good prediction is possible with the developed model with a predicted R2 value of 83.50%. Figure 4(b) shows the association among point angle, feed and thrust force. With higher point angle, thrust force tends to lower; with higher feeds, thrust forces rises significantly. Similarly, with higher drill speeds, thrust force tends to increase as presented in figure 4(c). Thrust force could be minimum for higher point angle and lower values of speed and feed as in figure 4(d).

3.2. Analysis of surface roughness

Surface texture and topography is the primary representative amid surface integrity properties and dimensions imparted by cutting tool employed in finishing process. Conventionally, texture of surface is measured as an index for evaluating vibration, damage and wear of machine tools rather than measuring the component performance. In industrial scenario, Ra (arithmetic average) value from a stable process is considered [41]. The roughness of the drilled hole is analyzed to identify the parameters that influence the most. ANOVA table formulated for hole roughness during analysis is presented in table 4. It is identified that, the influence of point angle (84.34%) is higher, followed by speed (9.69%) and feed (4.18%) towards the roughness of hole [43]. The ANOVA model is formulated with an R2 value of 98.21%, which satisfies the 95% confidence interval (CI) adopted during statistical analysis [44]. With p-value less than 0.05, point angle, feed rate and drill speed are found to be significant model terms. With adequate precision of 42.199, a lower noise levels (external disturbances) is observed during experimentation.

In actual versus predicted value graph shown in figure 5(a), along the 45° straight diagonal line, the data points are evenly scattered and are close enough to the diagonal line and the prediction is better with the predicted R^2 value of 96.74%. From the response 3D surface graph drawn between point angles, feed rate and surface roughness as presented in figure 5(b), with increase in point angle, surface roughness decreases and a similar trend is observed for higher rate of feed, where roughness value is lower for higher feed rate. When drill speed is considered, increase in drill speed leads to higher surface roughness as more amount of material is

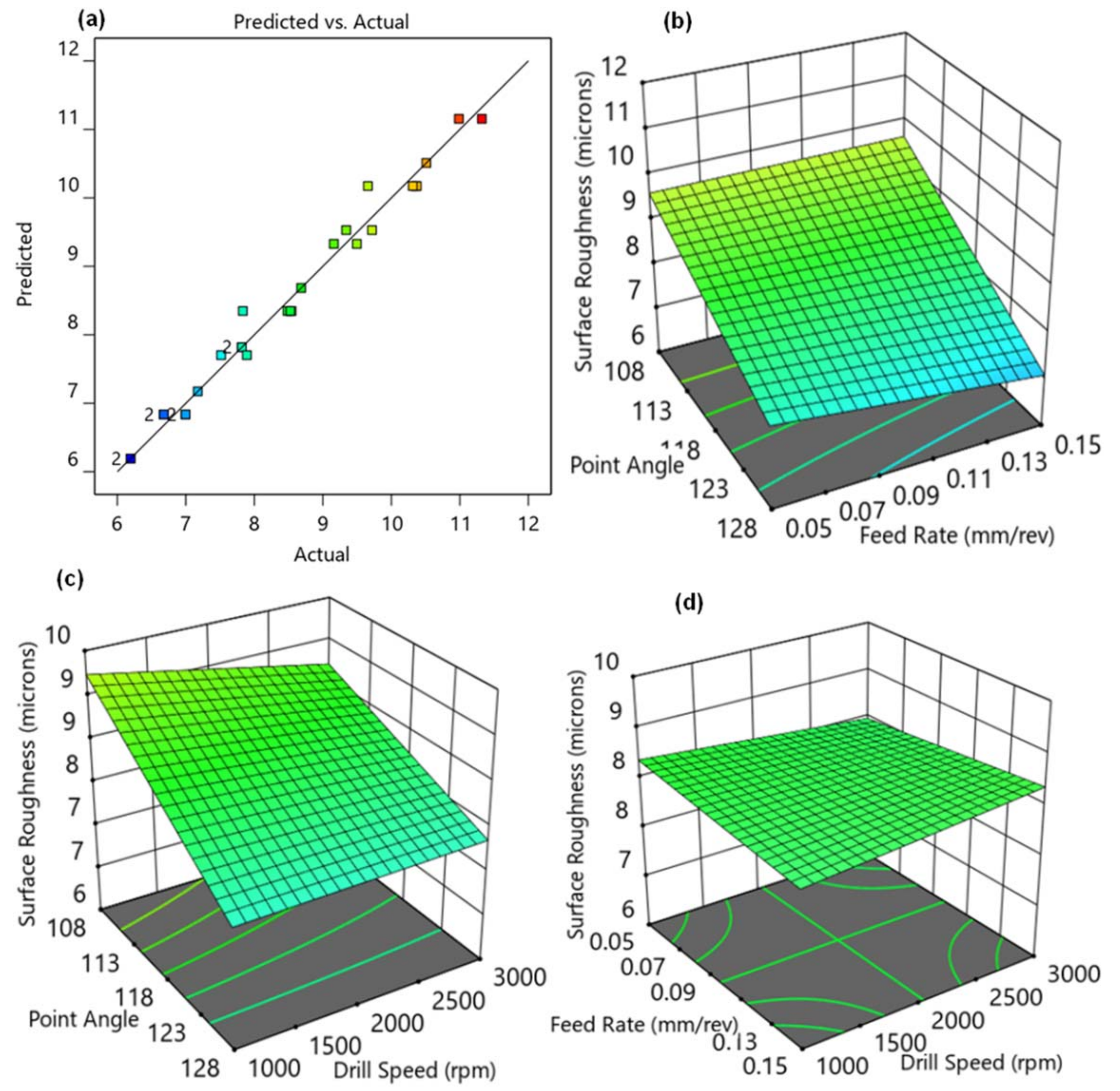

Figure 5. Diagnostic and model graphs for surface roughness.

removed during hole making as represented in figure 5(c). Figure 5(d) shows the relationship between feed rate, drill speed and roughness. The roughness value inside the drilled hole is minimum for higher point angle and feed rate along with lower drill speed.

3.3. Analysis of roundness error

The performance of rotary mechanical parts motion is mainly affected by the shape or geometrical error known as roundness error. The roundness error rises considerably with feed rate [45]. The roundness error arises due to the generation of burrs at the exit and entry of drilled hole, and also because of dynamic uncertainty of drilling tool and rapid thrust force. A larger thrust force because of higher rate of feed can be the foremost reason for higher roundness error [46].

Table 5 presents the ANOVA analysis results for roundness error, where a significant model is developed with an R2 value of 90.70%. It is identified that, roundness error is highly influenced by point angle, whose contribution is 42.39%, feed rate by 33.58% [47] and drill speed by 14.72%.

Figure 6(a), presents the diagnostic plot of actual versus predicted plot, where all the experimental values and predicted values tend to lie scattered on both sides of the 45° straight diagonal line and a perfect fit is not possible in this case as the points are away from the diagonal line which is also supported by a low predicted R2 value of 83.05%. The 3D surface plot of roundness error drawn between feed and point angle is presented in figure 6(b), which presents that with increase in point angle, roundness error tends to increase due to the wider cutting edges available in the drill bit. Similarly, with higher rate of feed, roundness error also tends to be higher due to higher volume of removing material during hole formation. A similar trend is observed for increasing speed; increasing

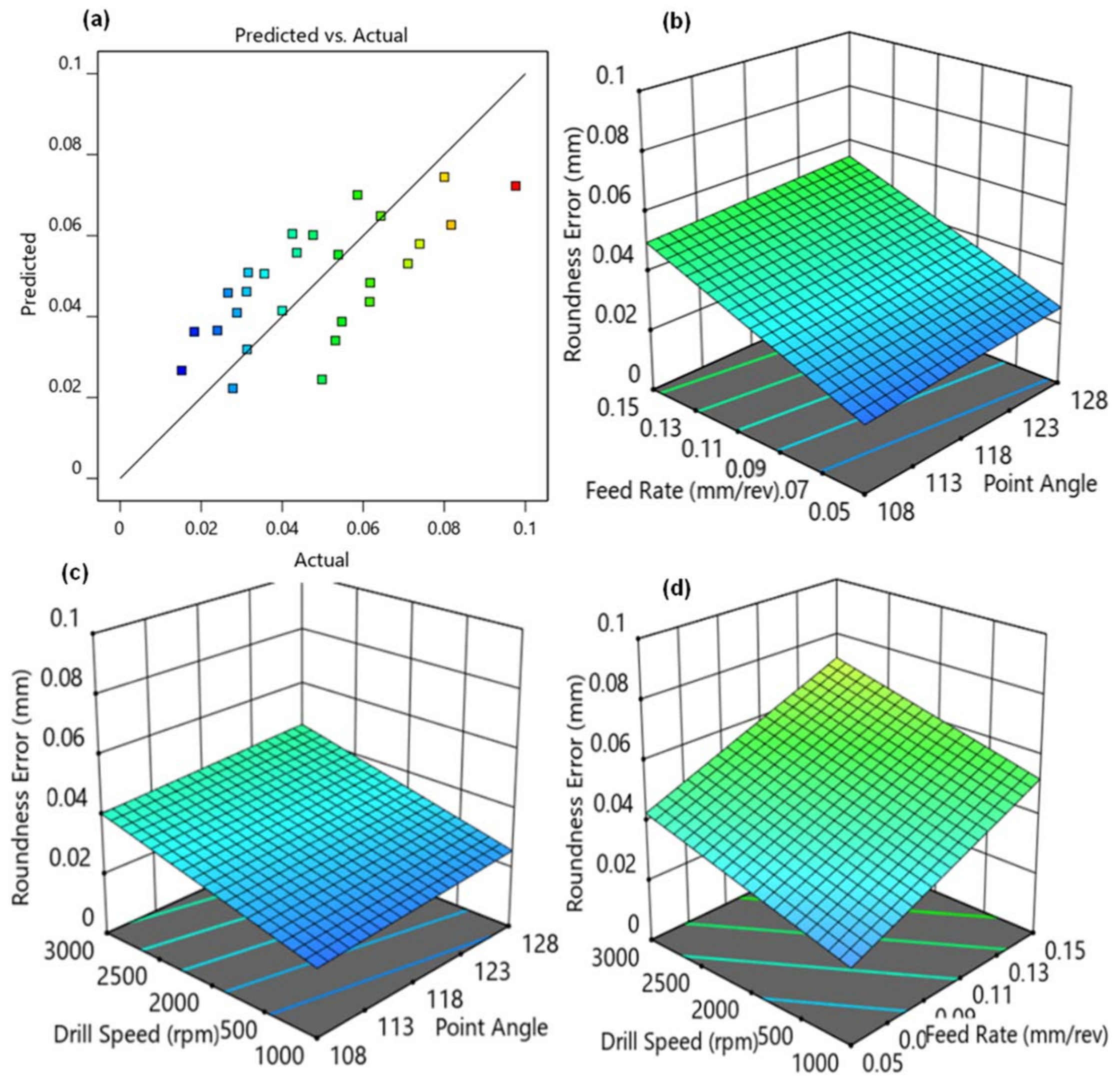

Figure 6. Diagnostic and model graphs for roundness error.

Table 5. ANOVA table for roundness error.

Source	SS	DoF	MS	F-value	p-value	
Model	0.010468	6	0.001745	32.51715	2.67E-09	significant
Point Angle	0.004892	2	0.002446	45.59439	3.55E-08	
Feed Rate	0.003876	2	0.001938	36.11944	2.3E-07	
Drill Speed	0.001699	2	0.00085	15.83762	7.54E-05	
Residual	0.001073	20	5.37E-05			
Cor Total	0.011541	26	R^2	0.907021		
Std. Dev.	0.007325		Adjusted R^2	0.879128		
Mean	0.048367		Predicted R^2	0.830546		
C.V.%	15.14422		Adeq Precision	20.99431		

the speed increases the roundness error as seen from figure 6(c). From figure 6(d) it is obvious that, lower feed rate and lower drill speed produces lower roundness error along with lower point angle.

3.4. Multi-objective constrained optimization using desirability approach

In multi-criteria optimization, all the output responses are considered and a common optimal condition is evolved (Reddy et al 2020). More than one response is considered simultaneously for building a suitable model with response surface for individual outputs and then finding a suitable operating state so that all responses are optimized within the desired ranges. The approach of desirability function is one among the most prevalent

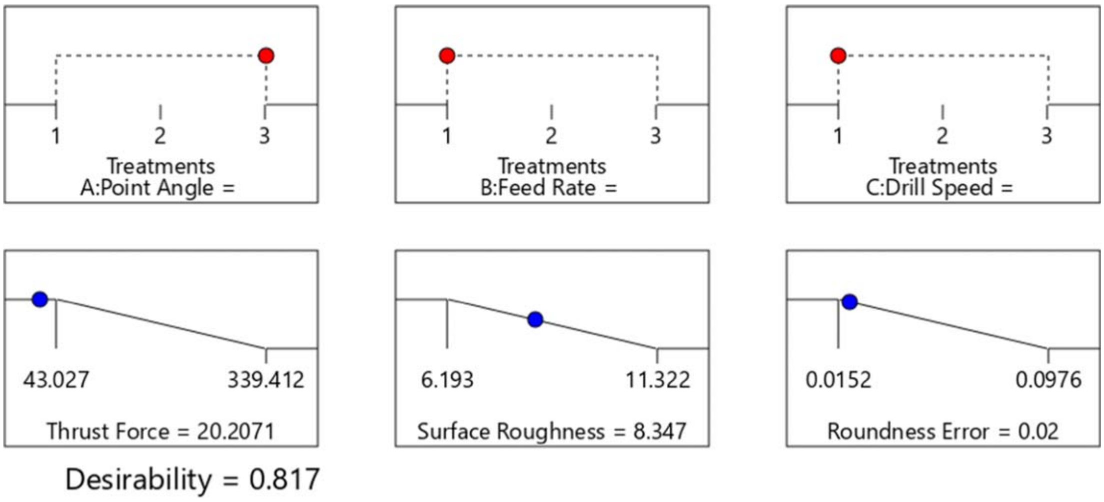

Figure 7. Desirability plot for unconstrained multi objective optimization.

approaches employed in optimizing multiple-responses. During implementing desirability, values that falls in between the probable values of 1 and 0 will be assigned by the desirability function where 1 represent the desirable or ideal value and 0 represent the non-desirable outcome [48].

$$d_r^{\max} = \begin{cases} 0 & \text{if } f_r(X) < A \\ \left(\dfrac{f_r(X) - A}{B - A}\right)^S & \text{if } A \leqslant f_r(X) \leqslant B \\ 1 & \text{if } f_r(X) > B \end{cases}$$

$$d_r^{\min} = \begin{cases} 1 & \text{if } f_r(X) < A \\ \left(\dfrac{f_r(X) - B}{B - A}\right)^S & \text{if } A \leqslant f_r(X) \leqslant B \\ 0 & \text{if } f_r(X) > B \end{cases}$$

$$D = \left(\prod_{r=1}^{R} d_r\right)^{1/R} \tag{1a}$$

The formulae to calculated desirability for minimization and maximization of responses are provided in equation (1), where A and B are extreme limits of selected inputs and the exponent S governs the weightage towards attaining the value of target; the input vector is X, and fr is the prediction model used and R is the number of desirability functions (responses) considered in the study [49].

In unconstrained optimization procedure, the prime objective is minimization of thrust force, surface roughness and roundness error. During simultaneous optimization using desirability, it is identified from the ramp plot (figure 7) that, the optimal input conditions are 128°point angle, 0.05 mm rev^{-1} of fee, 1000 rpm of speed with predicted outputs responses; thrust force of 20.207 N, roughness of 8.347 microns and roundness error of 0.02 mm with a desirability value of 0.817, which is nearer to the ideal value of 1.

In most of the industrial need, a perfect hole is needed from assembly point of view. Hence, a constrained optimization is performed with an objective of minimizing roughness and thrust force with roundness error as constrained (⩽0.05 mm). During optimization, thrust force and roughness is set as minimum and roundness error is set as target (0.05 mm). The optimal condition evolved is: 118°-point angle, 0.05 mm rev^{-1} of feed and 1000 rpm speed. The predicted outputs are: thrust force of 85.89 N, surface roughness of 6.837 microns and roundness error of 0.05 mm, as observed from ramp plot presented in figure 8. The thrust force and surface roughness values predicted are lower than that of the unconstrained optimization predicted values. The desirability value of constrained optimization is obtained as 0.872, which is also higher, when compared with unconstrained optimization.

Figure 9 presents interaction plot obtained during constrained optimization, showing the relationship between point angle and feed rate with desirability and other output responses for a drill speed of 1000 rpm. In the plot, the red color line represents feed rate of 0.05 mm rev^{-1}, green color represents 0.10 mm rev^{-1} feed rate and 0.15 mm rev^{-1} feed rate is represented by blue color. In interaction plot, if the relationship between two inputs over the considered output is characterized with parallel lines, interaction effect is null among the

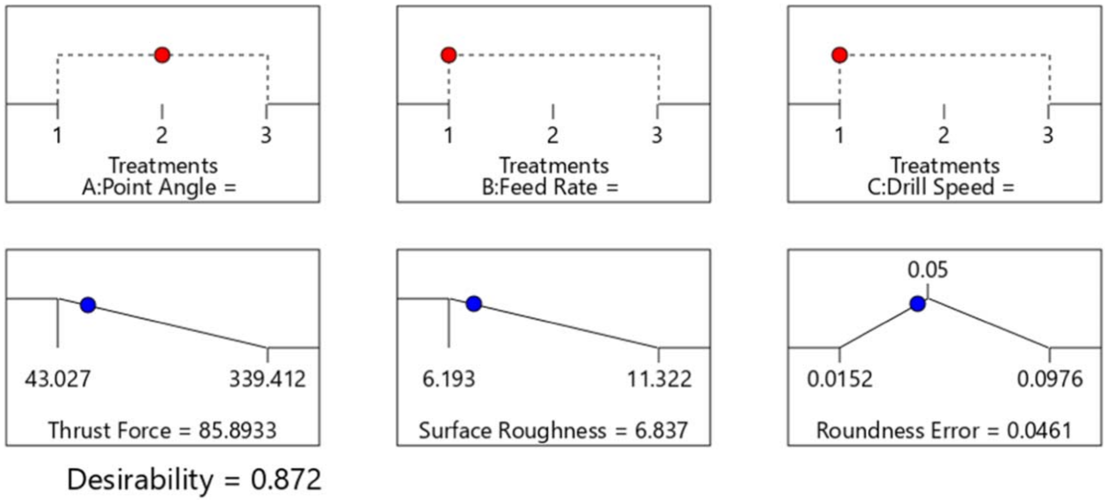

Figure 8. Desirability plot for constrained multi objective optimization.

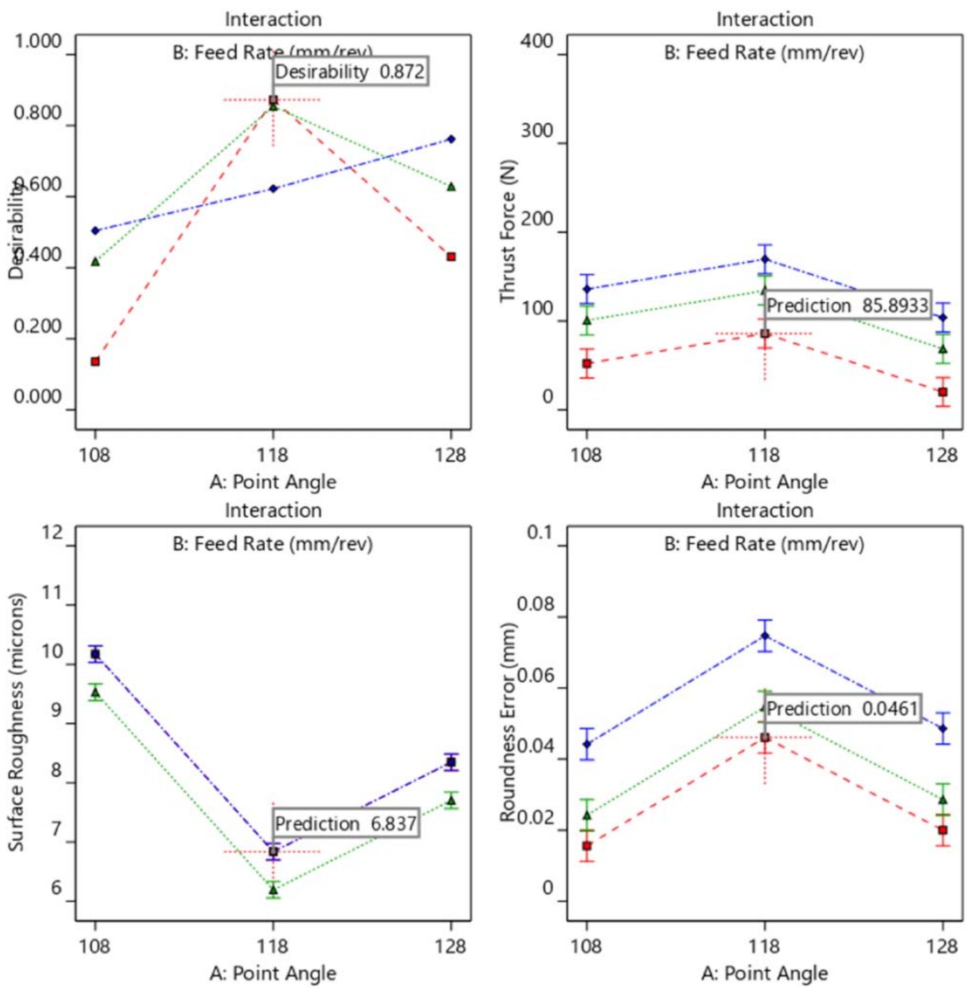

Figure 9. Interaction plot for desirability and output responses.

considered variables. But if the association is characterized by non-parallel lines, noteworthy relationship occurs among the considered inputs [12]. Among point angle and feed, no significant interaction exists; but for desirability a substantial relationship is seen among point angle and rate of feed.

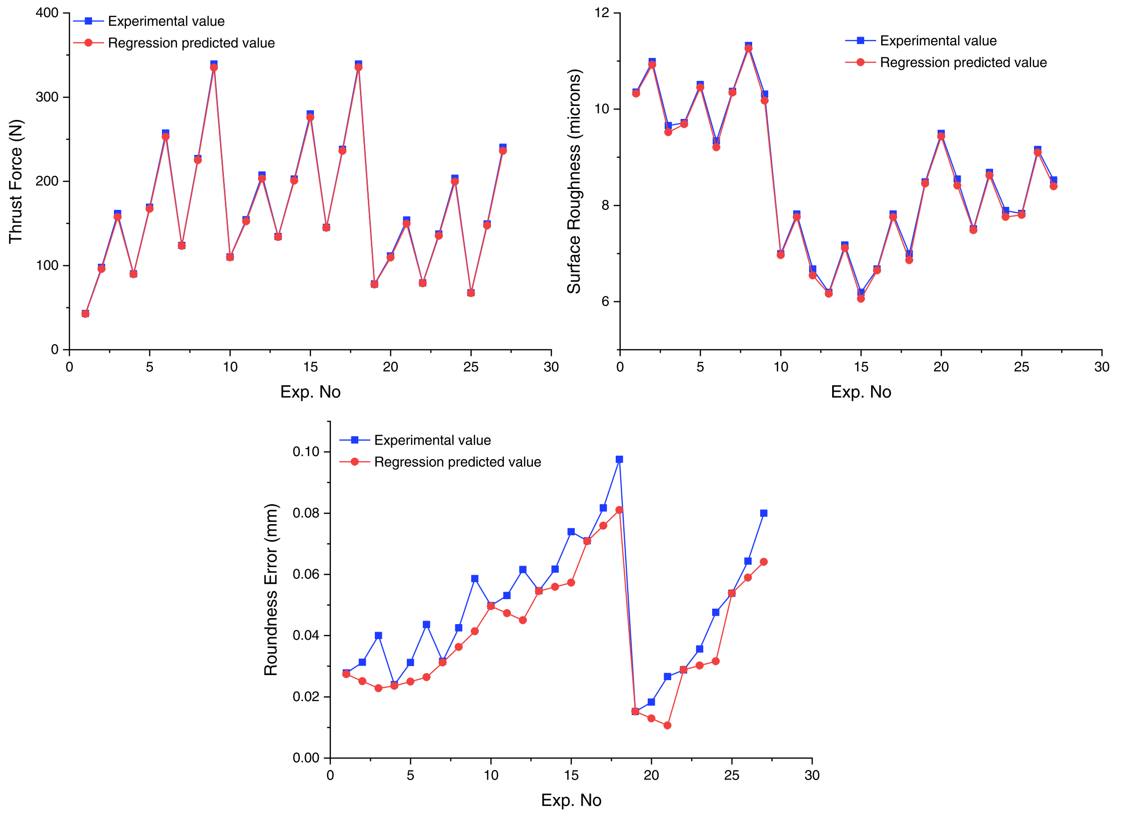

Figure 10. Comparing values from experiment and regression.

3.5. Development of empirical model using multiple-linear regression models

A regression model involving higher than one regressor/input variable is known as multiple linear regression (MLR) model. MLR are extensions of simple linear regression. MLR model is generally considered as approximating or empirical functions that forms a definite relationship among dependent and independent variable with satisfactory estimation to the unknown true function [50]. For predicting the outputs, empirical models are framed for individual output by adopting multiple linear regression (MLR) technique [51] for thrust force, surface roughness and roundness error as represented in equations (2)–(4). By using this developed model, prediction is done and comparison is done withthe experimental values, as shown in figure 10. With higher predicted R2 value, close prediction is possible and with lower predicted R2 value, a better prediction is not possible as seen from the result of roundness error.

$$\begin{aligned} Thrust\ Force &= -7453.34 + 122.287 \times P + 5775.12 \times F + 0.132235 \\ &\times Speed - 45.5463 \times P \times F - 0.001065 \times P \times S + 0.483960 \\ &\times F \times S - 0.496631 \times P^2 - 2659.58 \times F^2 + 0.000004 \times S^2 \end{aligned} \quad (2)$$

$$\begin{aligned} Surface\ Roughness &= 355.1 - 5.814 \times P - 18.23 \times F + 0.001388 \times S \\ &-0.3360 \times P \times F + 0.000019 \times P \times S + 0.003180 \\ &\times F \times S + 0.02423 \times P^2 + 257.6 \times F^2 - 0.000001 \times S^2 \end{aligned} \quad (3)$$

$$\begin{aligned} Roundness\ Error &= -3.704 + 0.06531 \times P - 2.371 \times F - 0.000006 \times S \\ &+0.01740 \times P \times F - 0.000000 \times P \times S + 0.000074 \\ &\times F \times S - 0.000283 \times P^2 + 2.280 \times F^2 + 0.000000 \times S^2 \end{aligned} \quad (4)$$

3.6. Prediction of output responses through Neural Networks

Neural networks mimic the brain of human beings artificially by simulating their process of learning [52]. The artificially developed neuron will look alike the biological neurons and also functions in similar mode. The input information will be delivered to the neurons based on the weights of incoming data and is managed by the propagation function which sums the data values based on the weights of incoming functions [53]. With reference to a threshold value, the resulting data value will be compared by the adopted activation function. If the threshold value is exceeded the input value, neurons get activated and if not, it will be repressed. The activated neurons send signal to the outgoing values based on the weights assigned to all interconnected neurons and so

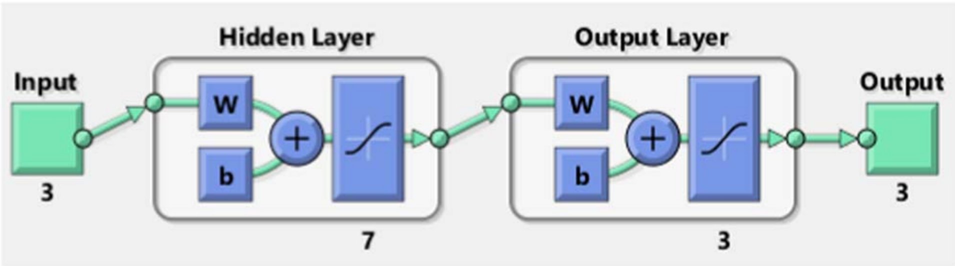

Figure 11. ANN architecture developed in MATLAB environment.

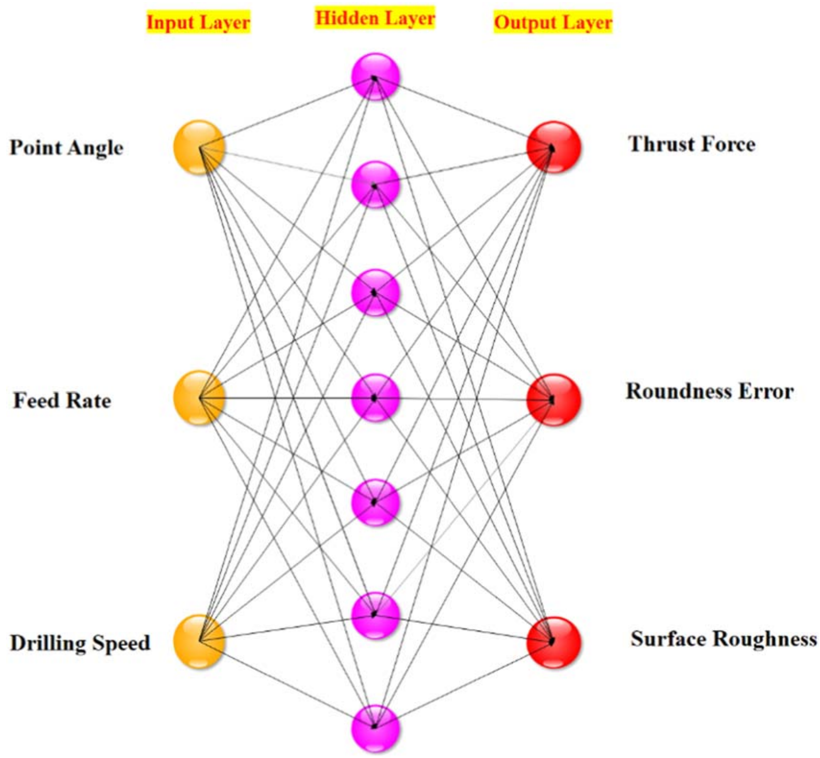

Figure 12. Neural network architecture.

forth. By deploying activation function (transfer function), the output signal transmitted by the neurons will be determined based on the weighted input. Generally, each and every neuron in a particular layer will be connected to the preceding and succeeding layer neurons except the output and input layer of the network. Transmission of data from a neuron in neural network is done layer by layer starting from input, hidden and output layer [54].

During training of neural network, if the output desired is known already, it is termed as supervisor learning or else it is unsupervised [55] after measuring the outputs related to the inputs, weights are changed to minimize the difference among desired and actual value of outputs. A common parameter, learning rate affects the speed of ANN towards arriving the model for better prediction [56]. For preventing the model from converging towards a saddle or local minima, momentum coefficient is used. The purpose ANN network is to predict the response for the provided input without doing expensive experimentation [57, 58].

During the process of developing a perfect ANN model, various networks are framed with different neurons in hidden layer, whereas the output neurons (3 responses) and input neurons (3 input parameters) are kept constant. Apart from changing the number of hidden layer neurons, momentum coefficient and learning rate are also changed to develop a perfect prediction model. Learning rate must be changed between the range of 0 to 1 whereas momentum coefficient must be changed between the values 0 to 2. In this present investigation, the ANN network developed is made up of 7 hidden layer neurons with optimal learning rate of 0.015 and 0.8 momentum coefficient towards achieving a better regression coefficient value. From the 27 trials, 21 data's are

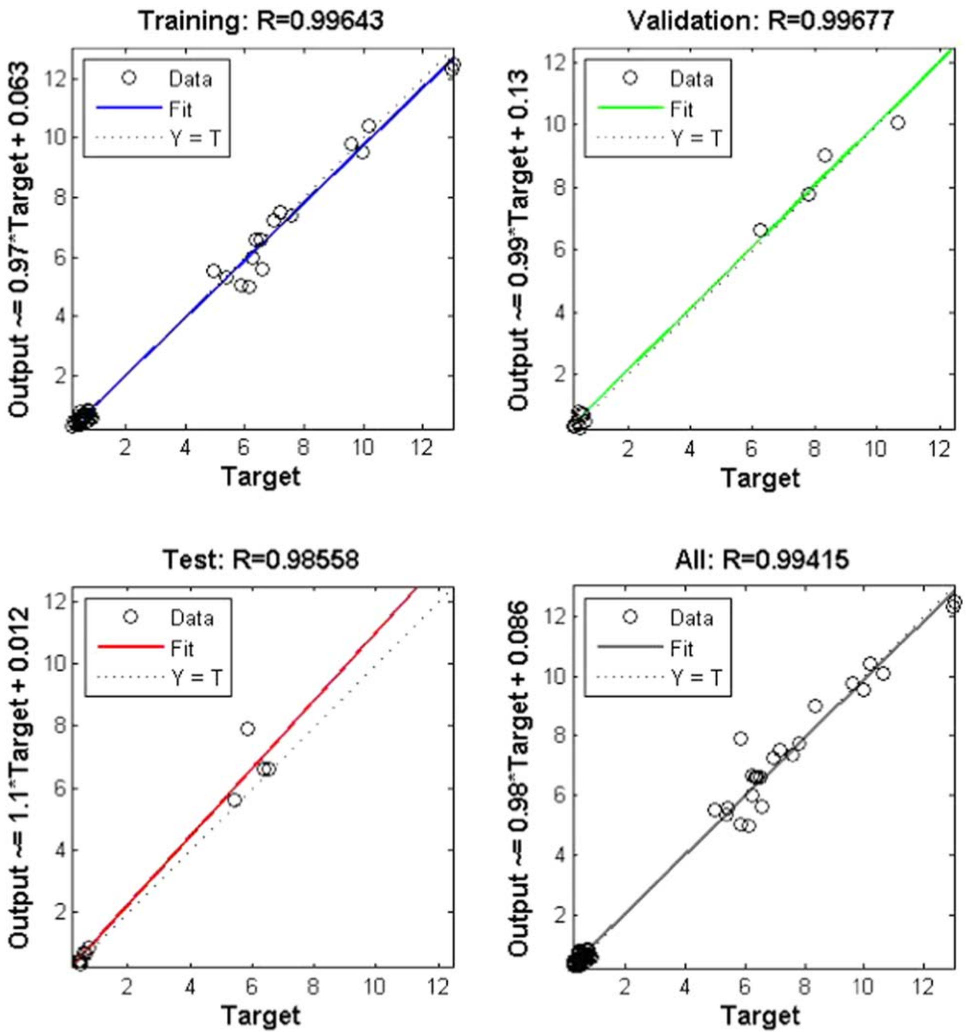

Figure 13. Regression plot obtained in ANN training.

used for ANN model training and the balance 6 trial data's are considered for testing ANN. Figure 11 presents the developed architecture of ANN in MATLAB and figure 12 shows the interconnectivity among the neurons from input layer, intermediate hidden layer and then to output layer.

Figure 13 presents the regression plot obtained during model development by ANN during training, validation, testing and in combined condition. The R^2 value obtained during training is 99.64%, 99.68% during validation check, 98.56% during testing and overall R^2 value obtained is 99.42%, which is close enough to the ideal value of 100%. The limitation encountered during development of ANN model is the time duration of training the ANN model for better prediction.

Mean squared error (MSE) variation during training of ANN model for an epoch (iteration) of 5000 is displayed in figure 14. It is observed that, MSE is lowest for the best, followed by training, validation and testing of ANN model. The confirmation value of 0.01224 is obtained during performance.

While training the developed model of ANN, during each epoch (iteration) validation check is performed towards comparing input and output predicted values. Gradient descent approach is adopted for minimizing the error function value by adjusting the weight factor in back-propagation feed forward neural network algorithm. Figure 15 presents the results from gradient value obtained during each epoch and validation check. The gradient value tends to lower towards zero during each iteration and finally, the gradient value gets stabilized without any further reduction.

Finally, after predicting the output responses through MLR models and ANN model, it is compared with the experimental values. Figure 16 presents comparison of predicted values with experimental condition for thrust force, figure 17 presents the comparison of surface roughness values and figure 18 compares the results of roundness error. It appears that, the prediction of outputs through ANN is closer enough to experimental values than MLR models due to the higher regression coefficient value. In conclusion, the ANN models outplay the MLR models for better prediction in this work.

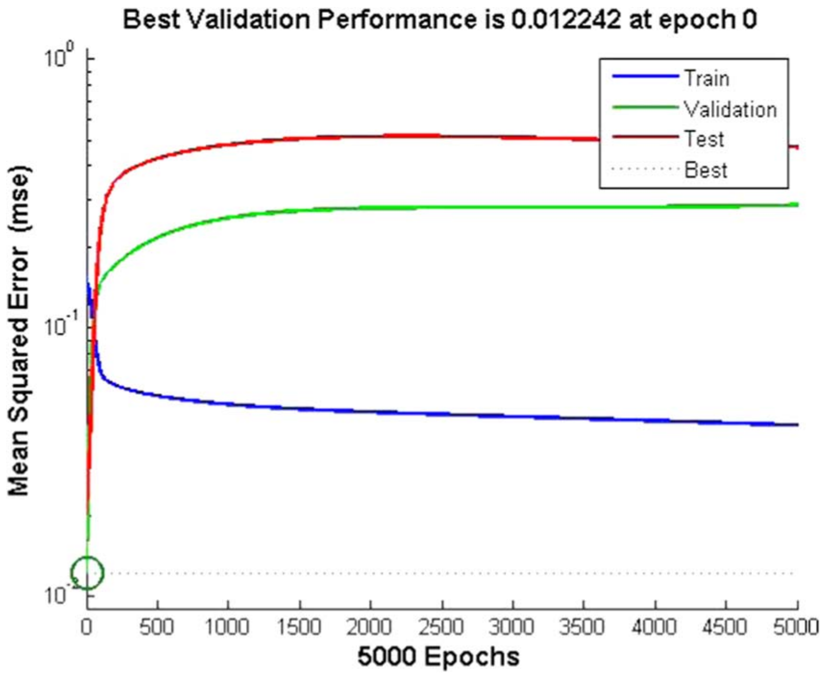

Figure 14. Performance plot attained from ANN training.

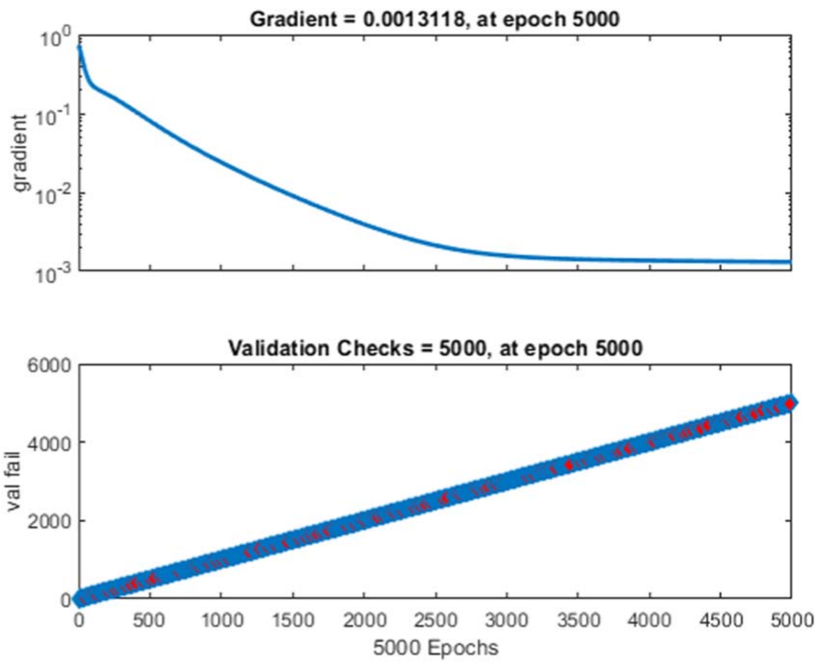

Figure 15. Training state obtained in ANN.

4. Conclusions

Various experiments are conducted for analyzing and developing models for roughness, thrust force and roundness error prediction in drilled holes on HAMMC. The following conclusions are made from the developed three different prediction models.

1. Stir casting is a low-cost method used to fabricate aluminium based composite with good distribution of particulates as seen from the SEM image. The tensile strength and micro-hardness of the HAMMC tends to increase when compared with as cast Al7075 alloy.

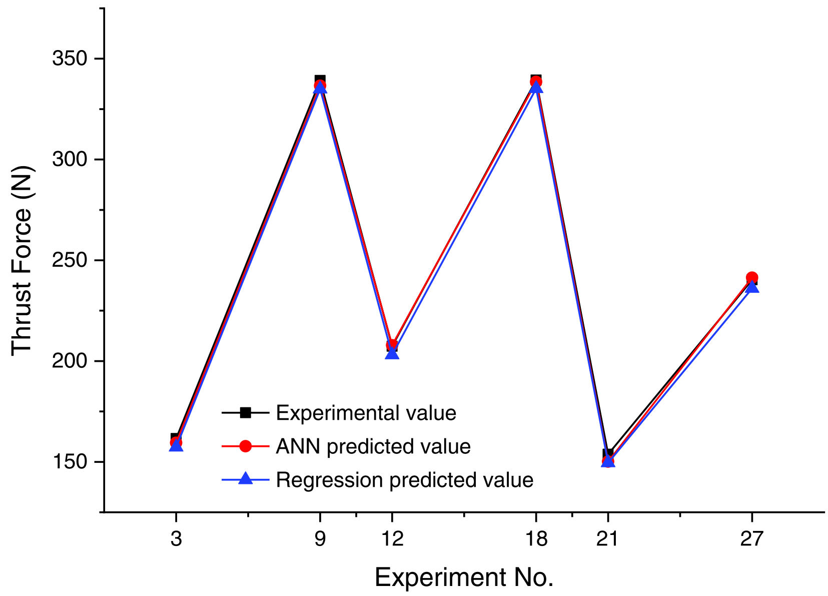

Figure 16. Comparing thrust force for experimental, regression and ANN values.

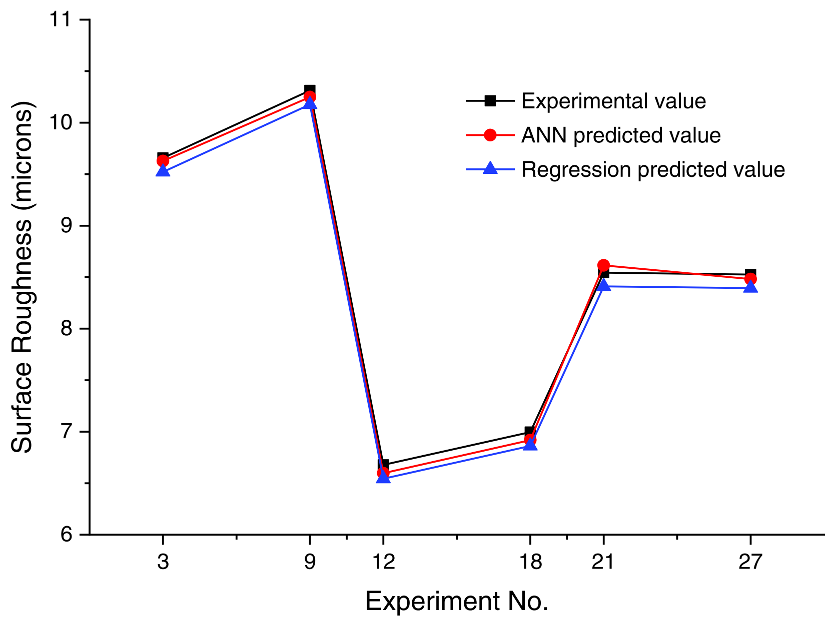

Figure 17. Comparing experimental, regressions and ANN predicted values for roughness.

2. For thrust force, the contribution of drill speed is 59.37% towards thrust force, 19.73% influence by feed rate and point angle by 12.06%. With increasing point angle, lower thrust force is sensed; with increasing rate of feed, thrust forces rises significantly. Similarly, with higher drill speeds, thrust force tends to increase.

3. Influence of point angle (84.34%) is higher, followed by drilling speed (9.69%) and feed rate (4.18%) towards hole roughness. Roughness decreases with higher point angle and feed rate, increase in drill speed leads to higher surface roughness as more amount of material is removed during hole making.

4. Roundness error is highly influenced by point angle, whose contribution is 42.39%, feed rate by 33.58% and drill speed by 14.72%.With higher point angle, roundness error tends to increase due to the wider cutting edges available in the drill bit. Similarly, with increment in feed rate and drill speed, roundness error also tends to be higher due to higher amount of material removal during hole generation.

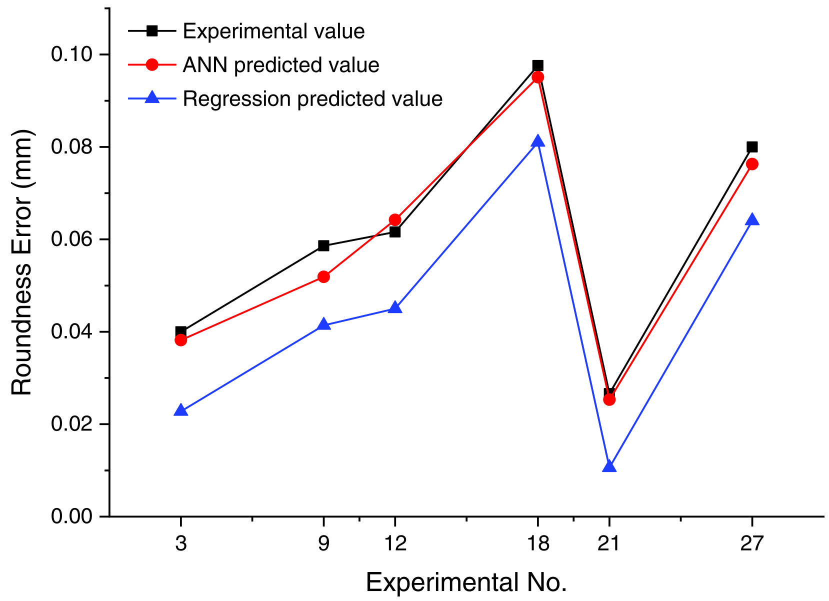

Figure 18. Comparing roundness error for experimental, regression and ANN values.

5. For unconstrained optimization, the optimal condition is: 128°-point angle, 0.05 mm rev^{-1} of feed and drill speed of 1000 rpm. Whereas for constrained optimization, the optimal condition is: 118°-point angle, 0.05 mm rev^{-1} feed and 1000 rpm of drill speed.

6. ANN model developed using back-propagation feed-forward network with gradient descent method predicts the output responses closer to the experimental results when compared with the second order polynomial equation generated using MLR models.

Data availability statement

All data that support the findings of this study are included within the article (and any supplementary files).

ORCID iDs

S Senthil Babu https://orcid.org/0000-0003-4300-2164
G Anbuchezhiyan https://orcid.org/0000-0001-7346-8876
Kumaran Palani https://orcid.org/0000-0002-7978-1617

References

[1] Hayajneh M T, Hassan A M, Mayyas A T and Alrashdan A 2011 Modeling the drilling process of some Al-Mg-Cu alloys and Al-Mg-Cu/SiC composites using artificial neural network *TOJSAT* **1** 18–24

[2] Gowda B U, Ravindra H V, Ullas M, Prakash G N and Ugrasen G 2014 Estimation of circularity, cylindricity and surface roughness in drilling Al-Si_3N_4 metal matrix composites using artificial neural network *Procedia Materials Science* **6** 1780–7

[3] Mayyas A, Qasaimeh A, Alzoubi K, Lu S, Hayajneh M T and Hassan A M 2012 Modeling the drilling process of aluminum composites using multiple regression analysis and artificial neural networks *Journal of Minerals and Materials Characterization and Engineering* **11** 1039

[4] Babu K A, Kumar G V and Venkataramaiah P 2015 Prediction of surface roughness in drilling of Al 7075/10%-SiCp composite under MQL condition using fuzzy logic *Indian Journal of Science and Technology* **8** 1

[5] Taskesen A and Kutukde K 2013 Analysis and optimization of drilling parameters for tool wear and hole dimensional accuracy in B_4C reinforced Al-alloy *Transactions of Nonferrous Metals Society of China* **23** 2524–36

[6] Rajmohan T, Palanikumar K and Kathirvel M 2012 Optimization of machining parameters in drilling hybrid aluminium metal matrix composites *Transactions of Nonferrous Metals Society of China* **22** 1286–97

[7] Okay F, Islak S and Turgut Y 2021 Investigation of machinability properties of aluminium matrix hybrid composites *J. Manuf. Processes* **68** 85–94

[8] Madhukar P, Selvaraj N and Rao C S P 2016 Manufacturing of aluminium nano hybrid composites: a state of review In *IOP Conf. Series: Materials Science and Engineering (Bristol)* (IOP Publishing) 149012114

[9] Zitoune R, Krishnaraj V, Almabouacif B S, Collombet F, Sima M and Jolin A 2012 Influence of machining parameters and new nano-coated tool on drilling performance of CFRP/Aluminium sandwich *Composites Part B: Engineering* **43** 1480–8

[10] Ramaswamy A and Perumal A V 2020 Multi-objective optimization of drilling EDM process parameters of LM13 Al allo$_{y-10}$ZrB_{2-5}TiC hybrid composite using RSM *Journal of the Brazilian Society of Mechanical Sciences and Engineering* **42** 1–18
[11] Sangeetha M, Vasanthaprabhu A, Sivaprakasam K, Nithya S, Dhinakaran V and Gunasekar P 2021 Surface roughness analysis for newly prepared CNT-coated metal matrix: RSM approach *Appl. Nanosci.* **11** 1–13
[12] Raj A M and Manoharan N 2014 Experimental investigation and analysis of torque in drilling Al–15% SiC–4% graphite metal matrix composites using response surface methodology *Indian Journal of Science and Technology* **7** 87–94
[13] Palanikumar K and Muniaraj A 2014 Experimental investigation and analysis of thrust force in drilling cast hybrid metal matrix (Al–15% SiC–4% graphite) composites *Measurement* **53** 40–250
[14] Adalarasan R and Santhanakumar M 2015 Application of Taguchi based response surface method (TRSM) for optimization of multi responses in drilling Al/SiC/Al_2O_3 hybrid composite *Journal of the Institution of Engineers (India): Series C* **96** 65–71
[15] Rubi C S and Prakash J U 2020 Drilling of hybrid aluminum matrix composites using grey-taguchi method *INCAS Bulletin* **12** 167–74
[16] Anbuchezhiyan G, Muthuramalingam T and Mohan B 2018 Effect of process parameters on mechanical properties of hollow glass microsphere reinforced magnesium alloy syntactic foams under vacuum die casting *Archives of Civil and Mechanical Engineering* **18** 1645–50
[17] Lalmuan S K, Das S, Chandrasekaran M and Tamang S K 2017 Machining investigation on hybrid metal matrix composites-a review *Mater. Today Proc.* **4** 8167–75
[18] Sharma N, Sharma V S, Sharma R C, Arora R and Sharma A 2022 Development of quality microholes by electrical discharge drilling on Al/SiC composite using of Grey-desirability approach *International Journal of Lightweight Materials and Manufacture* **5** 267–77
[19] Fenghong C, Chang C, Zhenyu W, Muthuramalingam T and Anbuchezhiyan G 2019 Effects of silicon carbide and tungsten carbide in aluminium metal matrix composites *Silicon* **11** 2625–32
[20] Ramadoss N, Pazhanivel K and Anbuchezhiyan G 2020 Synthesis of B4C and BN reinforced Al7075 hybrid composites using stir casting method *Journal of Materials Research and Technology* **9** 6297–304
[21] Anbuchezhiyan G, Mohan B, Senthilkumar N and Pugazhenthi R 2021 Synthesis and Characterization of Silicon Nitride Reinforced Al–Mg–Zn Alloy Composites *Met. Mater. Int.* **27** 3058–69
[22] Rajeswari B and Amirthagadeswaran K S 2017 Experimental investigation of machinability characteristics and multi-response optimization of end milling in aluminium composites using RSM based grey relational analysis *Measurement* **105** 78–86
[23] Tanwir Alam M 2021 Physical, corrosion and microstructural analysis of A356/SiC nanocomposites fabricated through stir casting process *Materials Science Forum* 1034 (Switzerland: Scientific.Net, Publisher in Materials Science and Engineering) 73–86 Trans Tech Publications Ltd.
[24] Juliyana S J and Prakash J U 2020 Drilling parameter optimization of metal matrix composites (LM5/ZrO_2) using taguchi technique *Mater. Today Proc.* **33** 3046–50
[25] Li J and Laghari R A 2019 A review on machining and optimization of particle-reinforced metal matrix composites *Int. J. Adv. Manuf. Technol.* **100** 2929–43
[26] Rubi C S, Prakash J U and Rajkumar C 2020 August. optimization of process parameters using taguchi technique for drilling aluminium matrix composites (LM6/B4C). In *IOP Conf. Ser.: Mater. Sci. Eng.* (Bristol: IOP Publishing) 912032016
[27] Jayakanth J J, Mamidi V K, Pugazhenthi R, Anbuchezhiyan G and Ponshanmugakumar A 2021 An investigation on wear properties of SiC/WC strengthened aluminium alloy hybrid composites *Mater. Today Proc.* **46** 3542–5
[28] Liu S, Wang Y, Muthuramalingam T and Anbuchezhiyan G 2019 Effect of B4C and MOS2 reinforcement on micro structure and wear properties of aluminum hybrid composite for automotive applications *Composites Part B: Engineering* **176** 107329
[29] Pugazhenthi R, Sreeram D, Scaria C T, Anbuchezhiyan G and Nanthakumar P 2021 Effect of process parameters on machining of Al-TiC metal matrix composites using RSM *Mater. Today Proc.* **46** 3282–7
[30] Karthikeyan S, Mohan B, Kathiresan S and Anbuchezhiyan G 2021 Effect of process parameters on machinability, hemocompatibility and surface integrity of SS 316L using R-MRAFF *Journal of Materials Research and Technology* **15** 2658–72
[31] Ayyandurai M, Mohan B and Anbuchezhiyan G 2021 Characterization and machining studies of nano borosilicate particles reinforced aluminium alloy composites using AWJM process *Journal of Materials Research and Technology* **15** 2170–87
[32] Anbuchezhiyan G, Mohan B and Muthuramalingam T 2019 Synthesis and characterization of nano-glass particles reinforced AZ91D magnesium alloy composites In*Advances in Materials and Metallurgy* (Singapore: Springer) 39–45
[33] Ramamurthy M, Balasubramanian P, Senthilkumar N and Anbuchezhiyan G 2022 Influence of process parameters on the microstructure and mechanical properties of friction stir welds of AA2014 and AA6063 aluminium alloys using response surface methodology *Mater. Res. Express* **9** 026528
[34] Akbari M and Asadi P 2019 Optimization of microstructural and mechanical properties of friction stir welded A356 pipes using Taguchi method *Mater. Res. Express* **6** 066545
[35] Akbari M and Asadi P 2021 Optimization of microstructural and mechanical properties of brass wire produced by friction stir extrusion using Taguchi method *Proc. Inst. Mech. Eng. Part L J. Mater. Des. Appl.* **235** 2709–19
[36] Reddy P V, Ramanjaneyulu P, Reddy B V and Rao P S 2020 Simultaneous optimization of drilling responses using GRA on Al-6063/TiC composite *SN Applied Sciences* **2** 1–10
[37] Vinayagam B K and Yogeshwaran M 2019 An experimental investigation of drilling Al/Sic/mica hybrid composites *Mater. Today Proc.* **16** 808–15
[38] Daniel S A A, Pugazhenthi R, Kumar R and Vijayananth S 2019 Multi objective prediction and optimization of control parameters in the milling of aluminium hybrid metal matrix composites using ANN and Taguchi-grey relational analysis. Defence *Technology* **15** 545–56
[39] Xavier L F and Suresh P 2018 Drilling studies on the prepared aluminum metal matrix composite from wet grinder stone dust particles *Science and Engineering of Composite Materials* **25** 473–87
[40] Krishnaiah K and Shahabudeen P 2012 *Applied design of experiments and taguchi methods* (New Delhi: PHI Learning)
[41] Rakesh P K, Singh I and Kumar D 2012 Drilling of composite laminates with solid and hollow drill point geometries *J. Compos. Mater.* **46** 3173–80
[42] Latha B, Senthilkumar V S and Palanikumar K 2011 Influence of drill geometry on thrust force in drilling GFRP composites *J. Reinf. Plast. Compos.* **30** 463–72
[43] Dehghan S, Ismail M I S, Ariffin M K A and Baharudin B T H T 2019 Measurement and analysis of thrust force and torque in friction drilling of difficult-to-machine materials *Int. J. Adv. Manuf. Technol.* **105** 2749–69
[44] Velavan K, Mohan B, Anbuchezhiyan G and Senthilkumar N 2021 Implications of SiC/Al2O3 reinforced Al-Mg-Zn alloy hybrid nano composites using vacuum sintering method *Silicon* **13** 3639–47

[45] Uddin M, Basak A, Pramanik A, Singh S, Krolczyk G M and Prakash C 2018 Evaluating hole quality in drilling of Al 6061 alloys *Materials* **11** 2443
[46] Palanikumar K, C Rubio J, Abrao A M, Esteves Correia A and Davim J P 2008 Influence of drill point angle in high speed drilling of glass fiber reinforced plastics *J. Compos. Mater.* **42** 2585–97
[47] Lachaud F, Piquet R, Collombet F and Surcin L 2001 Drilling of composite structures *Compos. Struct.* **52** 511–6
[48] Chaudhary G, Kumar M, Verma S and Srivastav A 2014 Optimization of drilling parameters of hybrid metal matrix composites using response surface methodology *Procedia Materials Science* **6** 229–37
[49] Ghoreishi R, Roohi A H and Ghadikolaei A D 2018 Analysis of the influence of cutting parameters on surface roughness and cutting forces in high speed face milling of Al/SiC MMC *Mater. Res. Express* **5** 086521
[50] Tamang S K and Chandrasekaran M 2015 Modeling and optimization of parameters for minimizing surface roughness and tool wear in turning Al/SiCp MMC, using conventional and soft computing techniques *Advances in Production Engineering & Management* **10** 59
[51] Saini P and Singh P K 2021 Optimization of end milling parameters for rough and finish machining of Al-4032/3% SiC metal matrix composite *Engineering Research Express* **3** 045009
[52] Rajmohan T, Palanikumar K and Harish G 2012 Surface roughness evaluation in drilling hybrid metal matrix composites. in emerging trends in science *Engineering and Technology* (India: Springer) 325–32
[53] Chaudhari M and Kumar M S 2018 Reinforcement and Cutting Tools Interaction during MMC Machining-a review *Nano Hybrids and Composites* **22** 47–54
[54] Subramanian A V M, Nachimuthu M D G and Cinnasamy V 2017 Assessment of cutting force and surface roughness in LM6/SiCp using response surface methodology *Journal of Applied Research and Technology* **15** 283–96
[55] Senthil Babu S and Vinayagam B K 2006 Thrust force, surface roughness and ovality prediction by rsm in drilling of aluminium based metal matrix composites *ARPN Journal of Engineering and Applied Sciences* **10** 7941–51
[56] Markopoulos A P, Pressas I S, Papantoniou I G, Karkalos N E and Davim J P 2015 *Modern Manufacturing Engineering* (*Machining and Machining Modeling of Metal Matrix Composites—A Review Part of the Materials Forming, Machining and Tribology*) (Switzerland: Springer, Cham) Ch 4 pp 99–141
[57] Kalyan Chakaravarthy V V, Rajmohan T, Vijayan D, Palanikumar K and Latha B 2020 Sustainable drilling performance optimization for Nano SiC reinforced Al matrix composites *Mater. Manuf. Processes* **35** 1304–12
[58] Xavier L F, Nelson D E S D S and Gnanaraj S 2015 Optimization of the surface roughness of the drilled holes on low cost reinforced aluminium metal matrix composite *International Journal of Applied Engineering Research* **10** 14809–20